

# A Soft-Switching of DC–DC Converter Based on a Phase-Shift-Controlled Active Boost Rectifier

Shivaleela<sup>1</sup>, Nagabhushan Patil<sup>2</sup>

<sup>1</sup>PG Student Department of EEE, PDA College of Engineering Kalaburgi-585102, India

<sup>2</sup>Associate Professor Department of EEE, PDA College of Engineering Kalaburgi-585102, India

**Abstract:** This paper proposes novel rectifiers named active boost rectifiers (ABRs) which are basically composed of a traditional diode rectifier and a bidirectional switch. However, the output voltage of the dc–dc transformer cannot be regulated. If the output voltage of a dc–dc transformer can be regulated high efficiency and high power density can be achieved. By adopting phase-shift control between the primary- and secondary-side switches, the output voltage regulation can be achieved when introducing the ABR to a dc–dc transformer. As a result, a soft-switching dc–dc converter is harvested. When the proposed converter operates in the soft-switching continuous conduction mode, zero-voltage switching (ZVS) performance for all the primary- and secondary side switches is achieved. When the converter operates in the discontinuous conduction mode, zero current switching (ZCS) for the primary-side switches and ZVS for the secondary-side switches are achieved. Furthermore, the diode reverse-recovery problem is alleviated by employing the ABR and phase-shift control scheme. As an example, the full-bridge converter with voltage-doubler ABR is analyzed to verify the proposed ABR concept and converters. The operation principles, voltage conversion ratio, and output Characteristics are analyzed in depth. Finally, experimental results are provided to verify the feasibility and effectiveness.

**Keywords:** Active boost rectifier (ABR), DC–DC converter, full-bridge converter (FBC), soft switching, voltage doubler (VD).

## 1. Introduction

This paper proposes the duty cycle of a dc–dc transformer, which is an open-loop controlled isolated dc–dc converter, is fixed at 50%. As a result, soft switching of all the power switches can be always achieved by utilizing the leakage or magnetizing inductance [1]. Therefore, high efficiency and high power density can be easily achieved. However, the output voltage/power of a dc–dc transformer cannot be regulated. If the output voltage of a dc–dc transformer can be regulated, high efficiency may be easily achieved. To achieve the goal mentioned previously, this paper proposes the active-boost-rectifier (ABR) concept. The ABR circuit is introduced to the dc–dc transformer topology to implement output voltage/power regulation. As a result, a family of wide-range soft-switching isolated dc–dc converters is harvested. The major advantage of the proposed converters is that the ZVS for all the active switches can be achieved in a wide load range. Most importantly, these converters can eliminate the reverse-recovery problem of rectifier diodes, which is very critical for high-efficiency applications. For further improvements on performance of efficiency, power density, and electromagnetic noise, many soft-switching dc–dc converters have been proposed for various applications to overcome the disadvantages in hard-switching dc–dc converters [2]–[3]. Among them, the phase-shift full bridge converter (FBC) is more attractive because it can achieve zero voltage switching (ZVS) for all the active switches by adopting phase-shift modulation. However, until now, it still suffers from high voltage ringing and reverse recovery on the secondary-side rectifier diodes, limited ZVS range, circulating current-related power loss, and duty cycle loss. The reverse recovery problem of the rectifier diodes becomes even more serious in high-output voltage and high-power applications. Various improvements have been proposed to solve these problems. Generally, some additional components are introduced to suppress the circulating currents and alleviate the reverse-recovery

problem. For instance, an auxiliary inductor, a transformer, or a winding is introduced to recycle the energy in [4]–[5]. In [5], two active switches are introduced to the secondary-side rectifier to solve the reverse-recovery problem, but the penalty is an additional conduction loss. Recently, the dual active bridge topology attracts great interest because it can realize ZVS for all the power switches [6]–[7]. But the limited ZVS range and high circulating currents at light load make this converter unsuitable for wide voltage/load range applications. Another attractive solution for the isolated dc–dc power conversion is the LLC resonant converter [8]–[9]. By designing and selecting a proper operation region, soft switching of all the active switches and rectifier diodes over a wide load range can be achieved with the LLC resonant converter.

However, frequency modulation makes the accurate modeling of the LLC converter difficult to achieve, and also complicates the design of magnetic components [10]. Besides, the resonant tank in the LLC converter should be designed carefully as well to achieve high efficiency, which remains a challenge for this type of converter.

## 2. Proposed DC-DC converter based on ABR

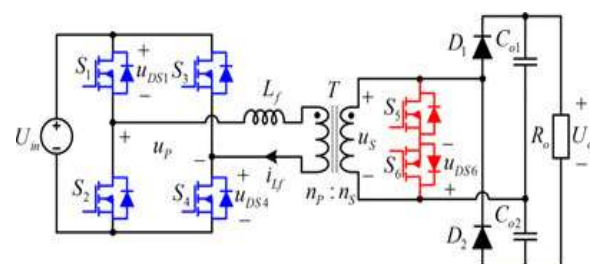


**Figure 1:** Proposed full-bridge converter with voltage-doubler active boost rectifier

The FBC-VD-ABR is shown in Figure 1, it consist of full bridge converter, active boost rectifier(ABR), which is

composed of the active bidirectional switch S5, S6 and diodes. Full bridge converters are mostly used in medium to high power applications. The output voltage can be controlled by the method called phase shift control. In phase shifted full bridge DC-DC converter, the switches attain zero voltage switching which reduces the switching losses and the converter can attain high efficiency at high switching frequencies. In topology shown in figure1, S1 and S4 are always turned-ON/OFF simultaneously, and the same with S2 and S3. A phase-shift angle between the primary- and secondary-side active switches is employed to regulate the output power and voltage.  $L_f$  stands for the total of the transformer leakage inductance and external inductor. The output series capacitors  $C_{o1}$  and  $C_{o2}$  have the same capacitance and are large enough to clamp the voltage stresses of the secondary-side switches and diodes to half of the output voltage.  $u_{DS1}$ ,  $u_{DS4}$ , and  $u_{DS6}$  are the drain to source voltages of S1, S4, and S6, respectively.  $u_p$  and  $u_s$  are the voltages on the primary side and secondary side of the transformer. And  $i_{lf}$  is the primary current flowing through the transformer. To simplify the analysis, the parasitic capacitance of MOSFET is ignored and the transformer is assumed to be ideal. The normalized voltage gain  $G$  is defined as

$$G = \frac{NU_o}{2U_{in}}$$

where  $U_{in}$ ,  $U_o$ , and  $N$  are the input voltage, output voltage, and transformer turns ratio  $n_p / n_s$ , respectively. The phase shift  $\phi$  is defined as the phase difference between S1 gate signal and S6 gate signal. Because this phase shift serves the same function as duty cycle in a PWM converter, we define duty cycle  $D$

$$D = \frac{\phi}{\pi}$$

According to the waveforms of the primary-side current, the converter has three operation modes, namely secondary side soft-switching continuous-conduction mode (SS-CCM), secondary-side hard-switching continuous-conduction mode (HS-CCM), and discontinuous conduction mode (DCM), respectively.

### 2.1 SS-CCM Operation

In SS-CCM, the converter can work in either the Buck mode ( $G < 1$ ), balance mode ( $G = 1$ ), or Boost mode ( $G > 1$ ). The key waveforms of the FBC-VD-ABR operating in SS-CCM are shown in Figure 2, where  $D_0$  is defined as the equivalent duty cycle during which the primary current returns to zero after the primary-side switches turn OFF, and  $T_s$  is the switching period. There are eight stages in one switching period. Due to the symmetry of the circuit, only four stages are analyzed here and corresponding equivalent circuits for each operation stage are shown in Figure 3.

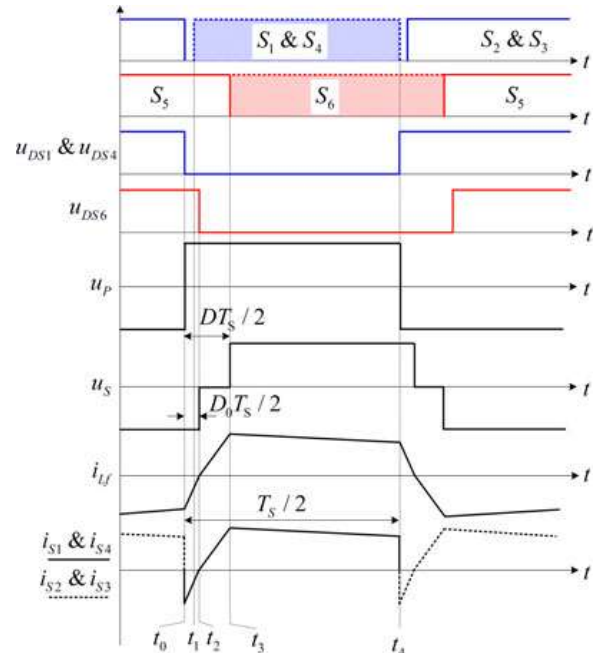


**Figure 2:** Key waveforms of the proposed converter in SS-CCM

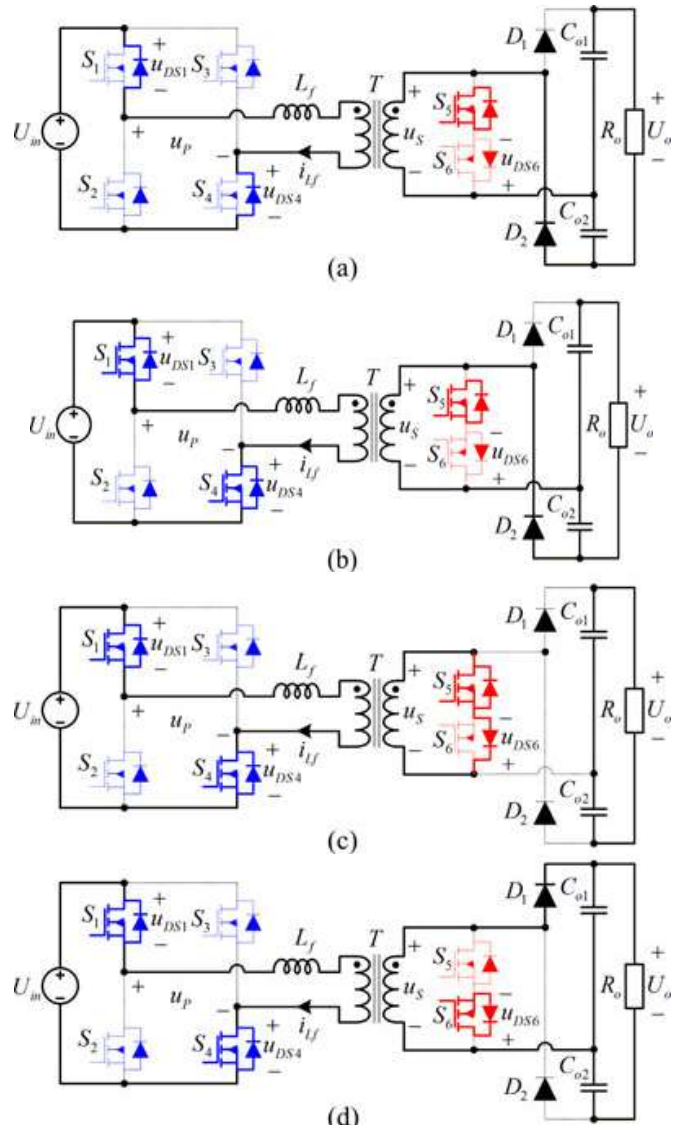


**Figure 3:** Equivalent circuits for each operation stage of SS-CCM: (a) Stage 1 [ $t_0, t_1$ ], (b) Stage 2 [ $t_1, t_2$ ], (c) Stage 3 [ $t_2, t_3$ ], and (d) Stage 4 [ $t_3, t_4$ ]

### 2.2 HS-CCM Operation

In SS-CCM, the secondary-side switches commute after  $i_{Lf}$  returns to zero, which means  $D > D_0$ . Once the secondary-side switches commute before  $i_{Lf}$  returns to zero with  $D < D_0$ , the converter will enter the HS-CCM, in which the converter can only work in the Buck mode ( $G < 1$ ). The key waveforms of the FBC-VD-ABR operating in HS-CCM are shown in Figure 4. There are also eight stages in one switching period, and the equivalent circuits for each operation stage are shown in Figure 5.

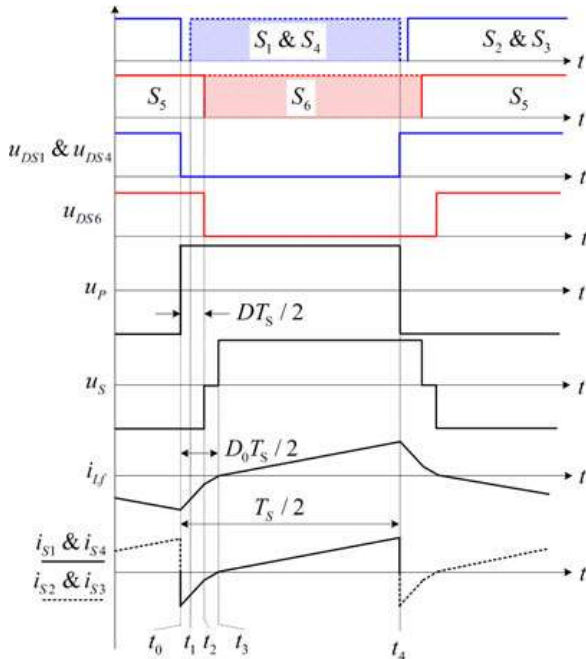


**Figure 4:** Key waveforms of the proposed converter in HS-CCM

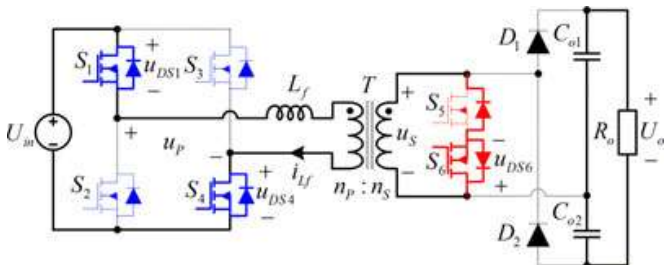


**Figure 5:** Equivalent circuit of Stage 3 in HS-CCM operation

### 2.3 DCM Operation

If the primary current has decreased to zero before the primary-side switches commute, the converter enters the DCM operation, in which the converter can only work in the Boost mode. The key waveforms of the FBC-VDABR operating in DCM are shown in Figure 6. There are also eight stages in one switching period. Due to the symmetry of the circuit, only four stages are analyzed here and corresponding equivalent circuits for each operation stage are shown in Figure 7.

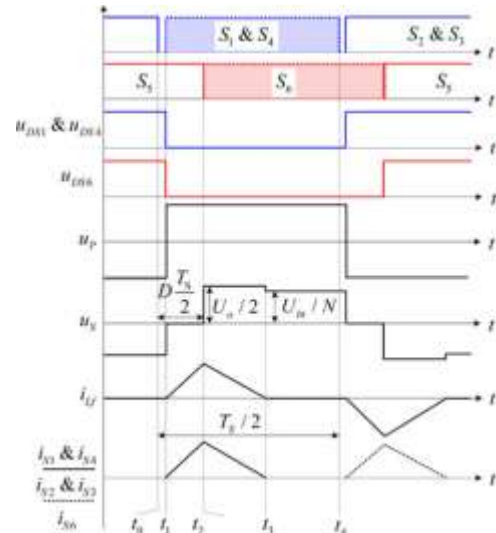


**Figure 6:** Key waveforms of the proposed converter in HS-CCM

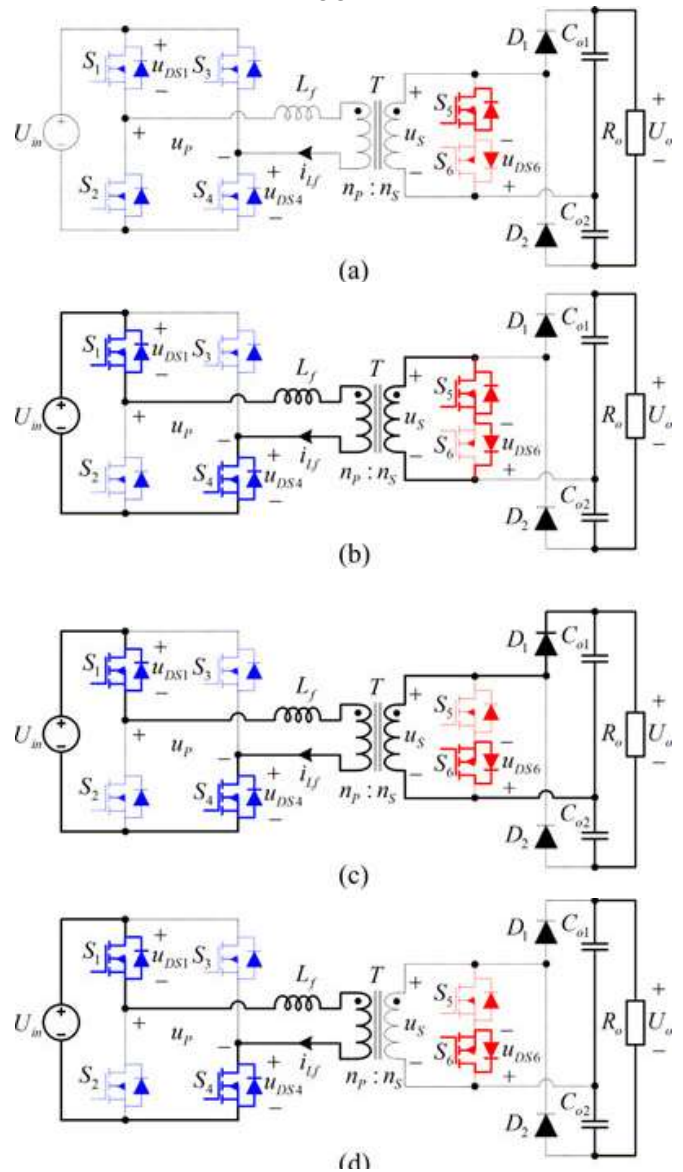


**Figure 7:** Equivalent circuits for each operation stage of DCM: (a) Stage 1 [ $t_0, t_1$ ], (b) Stage 2 [ $t_1, t_2$ ], (c) Stage 3 [ $t_2, t_3$ ], and (d) Stage 4 [ $t_3, t_4$ ]



### 3. Experimental Result

A 1 kW prototype controlled by a MC56F8247 digital signal processor is built to verify the theoretical analysis. The converter is designed for a stand-alone renewable power system, and used as the front-end converter of an inverter. The input voltage is 100–160 V, and the output voltage is 380V, when the converter works in the DCM, ZVS performance is lost while ZCS performance can be accomplished for the primary-side switches, and ZVS performance is achieved for the secondary side switches under the DCM. Since all the primary switches operate in the same pattern and both the two secondary-side switches operate symmetrically, ZCS and ZVS are accomplished for all the primary-side switches and secondary-side switches, respectively. When the input voltage is 160 V, the peak efficiency is about 96.4% and the efficiency at full load is about 95.8%. When the input voltage is 110 V, the maximum efficiency is about 95.3% and the efficiency at full load is about 94.6%. It can be seen that efficiency of more than 95% is achieved in a wide power and voltage ranges with the proposed converter.

### 4. Simulation Result

The simulation is being done in MATLAB/SIMULINK version 7.10.0.499(R2010a) for the proposed full-bridge converter with voltage-doubler active boost rectifier model is shown in Figure 8, by using 6 MOSFETs and 1 DC sources with  $v_{dc}$  as 160v shown in Fig.9. This converter gives an output voltage of 360v shown in Figure 11. The switching waveforms of the primary- and secondary-side switches under different operation modes are shown in Figure 10. The inductor voltage and current  $i_{Lf}$  waveforms of the FBC-VD-ABR under DCM, SS-CCM, and HSCCM, respectively. As shown in Figure 12, 13. Figure 14 shows the output voltage of the proposed FBC-VD-ABR under different input voltages.

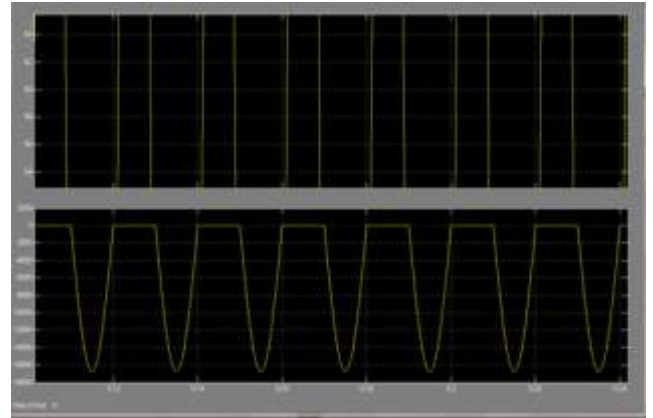


**Figure 9:** Input voltage and Input current

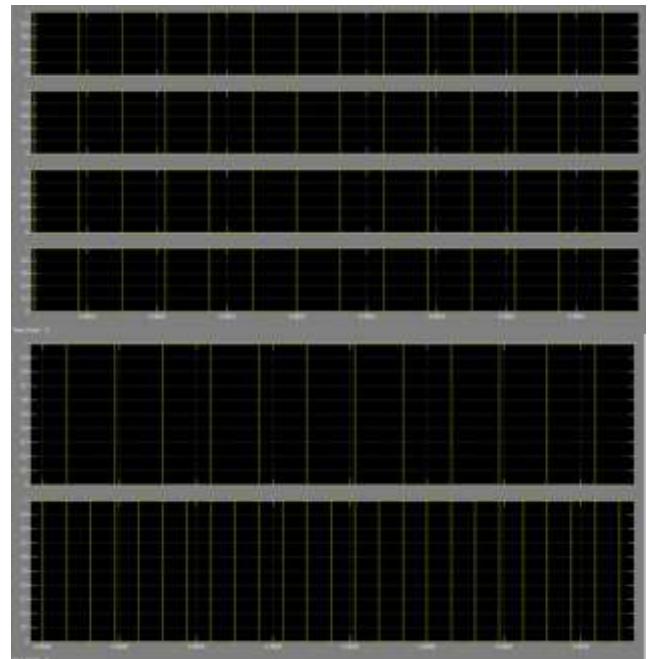


**Figure 10:** Switching pulse waveform

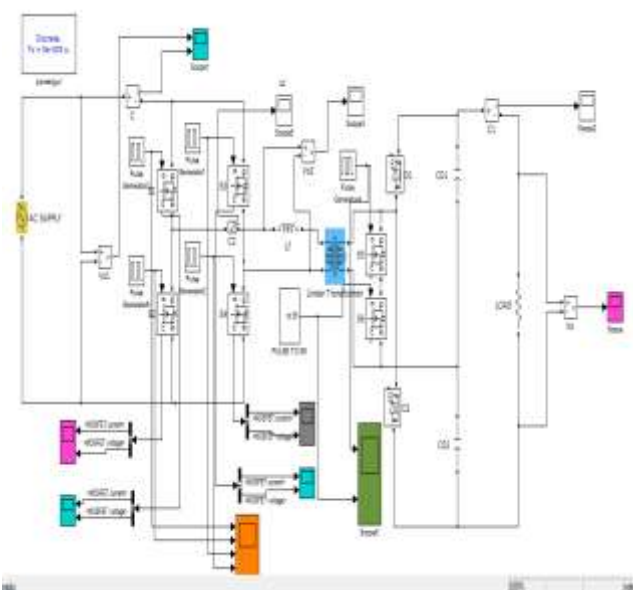


**Figure 8:** MATLAB/SIMULINK model of proposed full-bridge converter with voltage-doubler active boost rectifier

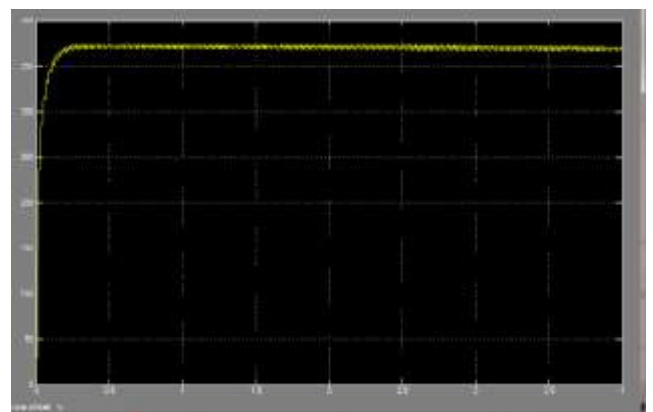


**Figure 11:** Output voltage

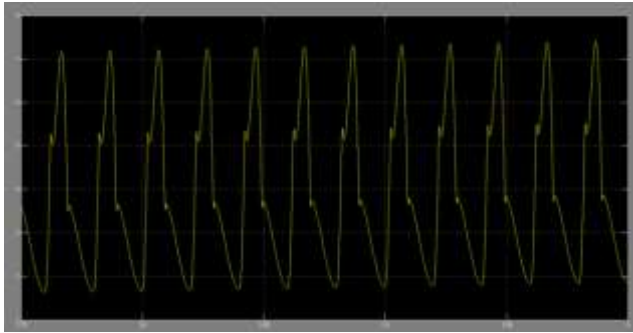


**Figure 12:** Inductor current

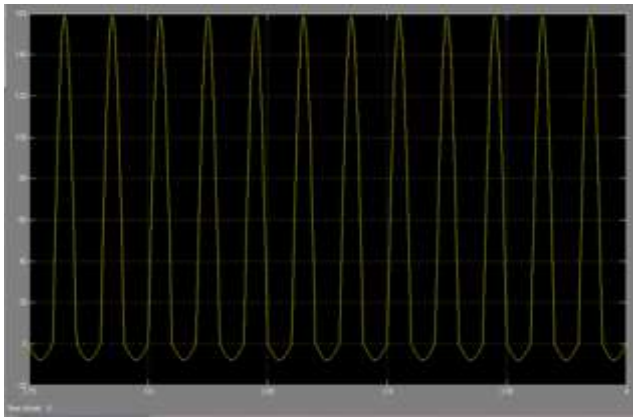


**Figure 13:** Inductor voltage

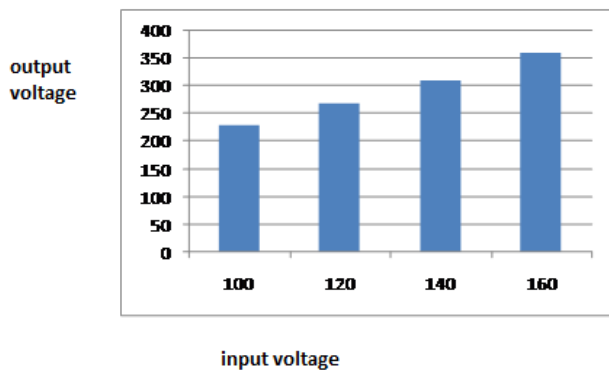


**Figure 14:** Input voltage versus Output voltage

## 5. Conclusion

In this paper, a family of soft-switching dc–dc converters has been presented for high-efficiency applications based on the novel proposed ABRs. In the proposed converters, all the power switches are operated at fixed 50% duty cycle, and the output voltage regulation is achieved by adopting phase shift control between the primary and secondary-side switches. ZVS performance has been achieved for both the primary- and secondary-side switches in a wide voltage and load range. Furthermore, the reverse-recovery problems associated with the rectifier diodes are alleviated. Therefore, the switching losses of the proposed converters can be reduced, which is important for high-frequency, high-efficiency, and high-power density applications. Moreover, the leakage inductance of the transformer has been utilized as the energy transfer inductor, and all the devices voltages are clamped to the input or output voltage. Thus, the voltage overshoots on the devices are effectively suppressed.

In addition, the proposed converters are suitable for wide-range applications because they can operate either in Buck or Boost mode and the FBC with VD ABR is analyzed with operation principles and output characteristics presented. Experimental results of a 1 kW prototype have verified the feasibility and effectiveness of the proposed topological methodology and converters.

## References

- [1] Y. Ren, M. Xu, J. Sun, and F. C. Lee, “A family of high power density unregulated bus converters,” *IEEE Trans. Power Electron.*, vol. 20, no. 5, . 1045–1054, Sep. 2005.
- [2] Y. S. Roh, Y. J. Moon, J. Park, and C.Yoo, “A two-phase interleaved power factor correction boost converter with a variation-tolerant phase shifting technique,” *IEEE Trans. Power Electron.*, vol. 29, no. 2, pp. 1032–1040, Feb. 2014.
- [3] Y. H. Kim, S. C. Shin, J. H. Lee, Y. C. Jung, and C. Y. Won, “Soft switching current-fed push-pull converter for 250-W AC module applications,” *IEEE Trans. Power Electron.*, vol. 29, no. 2, pp. 863–872, Feb.2014.
- [4] W. Yu, J. S. Lai, W. H. Lai, and H. Wan, “Hybrid resonant and PWM converter with high efficiency and full soft-switching range,” *IEEE Trans. Power Electron.*, vol. 27, no. 12, pp. 4925–4833, Dec. 2012.
- [5] T. Mishima, K. Akamatsu, and M. Nakaoka, “A high frequency-link secondary-side phase-shifted full-range soft-switching PWMDC–DC converter with ZCS active rectifier for EV battery charges,” *IEEE Trans. Power Electron.*, vol. 28, no. 12, pp. 5758–5773, Dec. 2013.
- [6] A. K. Jain and R. Ayyanar, “PWM control of dual active bridge: Comprehensive analysis and experimental verification,” *IEEE Trans. Power Electron.*, vol. 26, no. 4, pp. 1215–1227, Apr. 2011.
- [7] H. Koek, M. Neubert, and R. W. Doncker, “Enhanced modulation strategy for a three-phase dual active bridge—boosting efficiency of an electric vehicle converter,” *IEEE Trans. Power Electron.*, vol. 28, no. 12, pp. 5499–5507, Dec. 2013.
- [8] W. Feng, F. C. Lee, and P. Mattavelli, “Optimal trajectory control of LLC resonant converters for LED PWM dimming,” *IEEE Trans. Power Electron.*, vol. 29, no. 2, pp. 979–987, Feb. 2014.
- [9] X. Fang, H. Hu, F. Chen, U. Somani, E. Auadisian, J. Shen, and I. Batarseh, “Efficiency-oriented optimal design of the LLC resonant converter based on peak gain placement,” *IEEE Trans. Power Electron.*, vol. 28, no. 5, pp. 2285–2296, May 2013.
- [10] I. O. Lee and G. W. Moon, “The k-Q analysis for an LLC series resonant converter,” *IEEE Trans. Power Electron.*, vol. 29, no. 1, pp. 13–16, Jan.2014